AMERICAN SOCIETY FOR MICROBIOLOGY | Journal of Virology®

VACCINES AND ANTIVIRAL AGENTS

The Inhaled Steroid Ciclesonide Blocks SARS-CoV-2 RNA Replication by Targeting the Viral Replication-Transcription Complex in Cultured Cells

Shutoku Matsuyama,[a] Miyuki Kawase,[a] Naganori Nao,[a] Kazuya Shirato,[a] Makoto Ujike,[b] Wataru Kamitani,[c] Masayuki Shimojima,[d] Shuetsu Fukushi[d]

[a]Department of Virology III, National Institute of Infectious Diseases, Tokyo, Japan
[b]Faculty of Veterinary Medicine, Research Center for Animal Life Sciences, Nippon Veterinary and Life Science University, Tokyo, Japan
[c]Department of Infectious Diseases and Host Defense, Gunma University Graduate School of Medicine, Gunma, Japan
[d]Department of Virology I, National Institute of Infectious Diseases, Tokyo, Japan

ABSTRACT Here, we screened steroid compounds to obtain a drug expected to block host inflammatory responses and Middle East respiratory syndrome coronavirus (MERS-CoV) replication. Ciclesonide, an inhaled corticosteroid, suppressed the replication of MERS-CoV and other coronaviruses, including severe acute respiratory syndrome coronavirus 2 (SARS-CoV-2), the cause of coronavirus disease 2019 (COVID-19), in cultured cells. The 90% effective concentration (EC_{90}) of ciclesonide for SARS-CoV-2 in differentiated human bronchial tracheal epithelial cells was 0.55 μM. Eight consecutive passages of 43 SARS-CoV-2 isolates in the presence of ciclesonide generated 15 resistant mutants harboring single amino acid substitutions in nonstructural protein 3 (nsp3) or nsp4. Of note, ciclesonide suppressed the replication of all these mutants by 90% or more, suggesting that these mutants cannot completely overcome ciclesonide blockade. Under a microscope, the viral RNA replication-transcription complex in cells, which is thought to be detectable using antibodies specific for nsp3 and double-stranded RNA, was observed to fall in the presence of ciclesonide in a concentration-dependent manner. These observations indicate that the suppressive effect of ciclesonide on viral replication is specific to coronaviruses, highlighting it as a candidate drug for the treatment of COVID-19 patients.

IMPORTANCE The outbreak of SARS-CoV-2, the cause of COVID-19, is ongoing. New and effective antiviral agents that combat the disease are needed urgently. Here, we found that an inhaled corticosteroid, ciclesonide, suppresses the replication of coronaviruses, including betacoronaviruses (murine hepatitis virus type 2 [MHV-2], MERS-CoV, SARS-CoV, and SARS-CoV-2) and an alphacoronavirus (human coronavirus 229E [HCoV-229E]), in cultured cells. Ciclesonide is safe; indeed, it can be administered to infants at high concentrations. Thus, ciclesonide is expected to be a broad-spectrum antiviral drug that is effective against many members of the coronavirus family. It could be prescribed for the treatment of MERS and COVID-19.

KEYWORDS COVID-19, DMV, RTC, SARS-CoV-2, ciclesonide, coronavirus, steroid

The coronavirus disease 2019 (COVID-19) outbreak began in December 2019 in Wuhan, China (1). The causative virus, severe acute respiratory syndrome coronavirus 2 (SARS-CoV-2), spread rapidly worldwide and was declared a global health emergency by the World Health Organization. Thus, effective antiviral agents to combat the disease are needed urgently. Several drugs are effective against SARS-CoV-2 in cultured cells (2–4). Of these, remdesivir has undergone clinical trials in COVID-19

Citation Matsuyama S, Kawase M, Nao N, Shirato K, Ujike M, Kamitani W, Shimojima M, Fukushi S. 2021. The inhaled steroid ciclesonide blocks SARS-CoV-2 RNA replication by targeting the viral replication-transcription complex in cultured cells. J Virol 95:e01648-20. https://doi.org/10.1128/JVI.01648-20.

Editor Tom Gallagher, Loyola University Chicago

Address correspondence to Shutoku Matsuyama, matuyama@nih.go.jp.

Received 18 August 2020
Accepted 10 October 2020
Accepted manuscript posted online 14 October 2020
Published 9 December 2020

patients, with both positive and negative results (5, 6). Lopinavir/ritonavir and chloroquine/hydroxychloroquine are of no benefit (7, 8).

The virus can have inflammatory effects; therefore, steroids are used to treat severe inflammation, with beneficial effects in some cases. For example, high-dose steroids reduce symptoms in those with influenza encephalopathy (9). It would be highly beneficial if a virus-specific inhibitor was identified among the many steroid compounds that have been well characterized. However, systemic treatment with steroids is contraindicated in cases of severe pneumonia caused by Middle East respiratory syndrome coronavirus (MERS-CoV) or severe acute respiratory syndrome coronavirus (SARS-CoV); this is because steroids suppress innate and adaptive immune responses (10, 11), resulting in increased viral replication. In fact, for SARS (2003) and MERS (2013), systemic treatment with cortisone or prednisolone is associated with increased mortality (12, 13). Therefore, if steroid compounds are to be used to treat patients suffering from COVID-19, their tendency to increase virus replication must be abrogated. Here, we evaluated the antivirus effects of steroid compounds to reconsider their use for the treatment of pneumonia caused by coronavirus.

(This article was submitted to an online preprint archive [27].)

RESULTS

Antiviral effects of steroid compounds on MERS-CoV. Ninety-two steroid compounds chosen from the Prestwick Chemical Library were examined to assess the inhibitory effects of MERS-CoV-induced cytopathic effects. Vero cells treated with steroid compounds were infected with MERS-CoV at a multiplicity of infection (MOI) of 0.1 and then incubated for 3 days. Four steroid compounds, mometasone furoate, algestone acetophenide, ciclesonide, and mifepristone, conferred a $>$95% cell survival rate (Fig. 1a). Interestingly, a common structural feature of these compounds is a five- or six-membered monocycle attached to the steroid core. Indeed, three compounds (mometasone furoate, algestone acetophenide, and ciclesonide) have a similar structure in which the monocycle is attached at the cyclopentane ring of the steroid core via two parallel oxygen arms (Fig. 1b); this characteristic is not present in the other 89 steroid compounds tested in this study.

Next, we assessed the ability of eight steroid compounds (denoted by arrows in Fig. 1a) to suppress both the growth of MERS-CoV and virus-mediated cytotoxicity in Vero cells over a range of drug concentrations (0.1 to 100 μM). Ciclesonide exhibited low cytotoxicity and potent suppression of viral growth (Fig. 2a). Algestone acetophenide, mometasone, and mifepristone also suppressed viral growth; however, at 10 μM, the percent viability of cells treated with algestone acetophenide and mometasone was lower than that of cells treated with ciclesonide, and the ability of mifepristone and mometasone to suppress viral growth was lower than that of ciclesonide. Cortisone and prednisolone (which are used commonly for systemic steroid therapy), dexamethasone (which has strong immunosuppressant effects), and fluticasone (a common inhaled steroid drug) did not suppress viral growth (Fig. 2a). A time-of-addition assay to compare the viral inhibition efficacies of the steroids with those of E64d, a cathepsin-dependent virus entry inhibitor, and lopinavir, a viral 3CL protease inhibitor previously reported for SARS-CoV (14, 15), demonstrated that ciclesonide functions at the early stage of viral RNA replication (after the virus has entered the cell) (Fig. 3).

The antiviral effects of mometasone and ciclesonide against various viral species were tested by quantifying propagated virus in the culture medium of infected cells. Ciclesonide and mometasone suppressed the replication of murine hepatitis virus type 2 (MHV-2), MERS-CoV, SARS-CoV, human coronavirus 229E (HCoV-229E), and SARS-CoV-2 (all of which have a positive-strand RNA genome) but did not affect the replication of respiratory syncytial virus (RSV) or influenza virus (which have a negative-strand RNA genome) (Fig. 2b). In addition, ciclesonide slightly, but significantly, inhibited the replication of rubella virus (which has a positive-strand RNA genome) (Fig. 2b).

Identification of the target of ciclesonide during MERS-CoV replication. In an attempt to identify a druggable target for viral replication, we performed 11 consec-

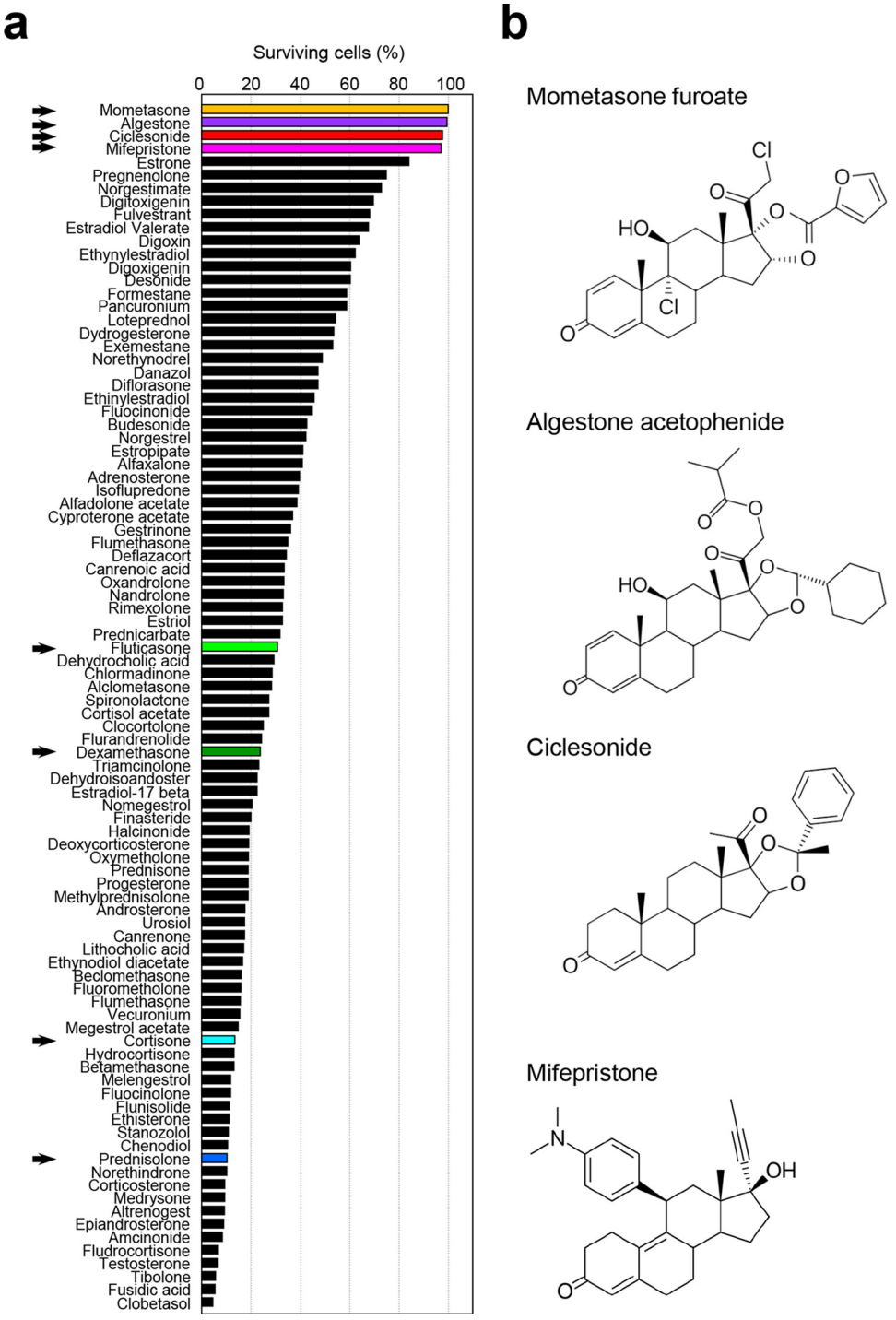

FIG 1 Steroid compounds reduce death rates of MERS-CoV-infected cells. (a) Cell survival. Vero cells seeded in 96-well microplates were infected with 100 50% tissue culture infective doses ($TCID_{50}$) of MERS-CoV in the presence of steroid compounds (10 μM). Cytopathic effects were observed at 72 h postinfection. Surviving cells were stained with crystal violet, photographed, and quantified using ImageJ software. Data are presented as the averages from two independent wells. Arrows indicate the steroid compounds assessed further in this study. (b) Four steroid compounds. The structures of the steroid compounds that conferred a >95% cell survival rate are depicted.

utive passages of MERS-CoV in the presence of 40 μM ciclesonide or 40 μM mometasone. A mutant virus displaying resistance to ciclesonide (but no virus displaying resistance to mometasone) was generated. Viral replication in the presence of ciclesonide was confirmed by measuring the virus titer in the culture medium of

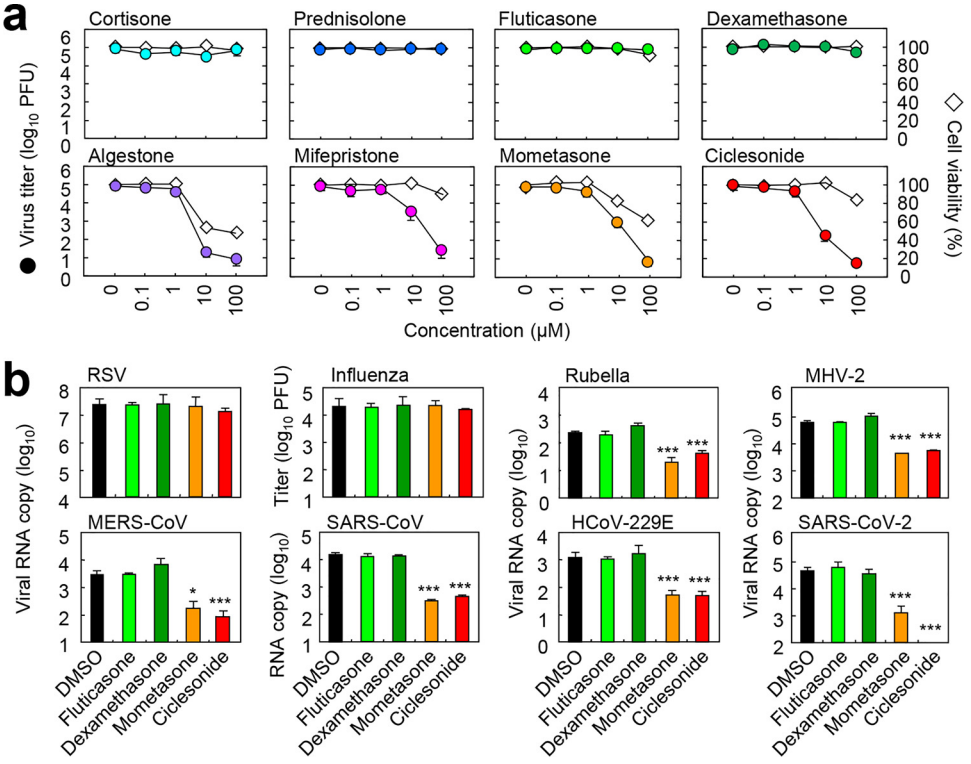

FIG 2 Steroid compounds suppress the replication of MERS-CoV and other viruses. (a) Effects of eight steroid compounds on MERS-CoV replication. Vero cells were infected with MERS-CoV at an MOI of 0.01 in the presence of the indicated steroids for 24 h. The viral titer in the cell supernatant was quantified by a plaque assay using Vero/*TMPRSS2* cells. Cell viability in the absence of virus was quantified by a WST assay. (b) Antiviral effects of steroid compounds on various viral species. Cells were infected with the indicated viruses at an MOI of 0.01 in the presence of dimethyl sulfoxide (DMSO) (control) or the indicated steroids. The viral yield in the cell supernatant was quantified by a plaque assay or real-time PCR. Hep-2 cells were incubated with respiratory syncytial virus A (RSV-A long) for 1 day; MDCK cells were incubated with influenza virus H3N2 for 1 day; Vero cells were incubated with rubella virus (TO336) for 7 days; DBT cells were incubated with murine coronavirus (MHV-2) for 1 day; Vero cells were incubated with MERS-CoV (EMC), SARS-CoV (Frankfurt-1), or SARS-CoV-2 (WK-521) for 1 day; and HeLa229 cells were incubated with HCoV-229E (VR-740) for 1 day. Data are presented as the means ± standard deviations from four independent wells. *, $P \leq 0.05$; ***, $P \leq 0.001$.

infected Vero cells at 24 h postinfection (hpi), along with the amount of viral RNA in infected cells at 6 hpi (Fig. 4a and b). Next-generation sequencing revealed that an amino acid substitution at A25V (C19647T in the reference sequence under GenBank accession number NC_019843.3 in nonstructural protein 15 [nsp15], a coronavirus endoribonuclease) (16–18) was predicted to cause resistance to ciclesonide. Subse-

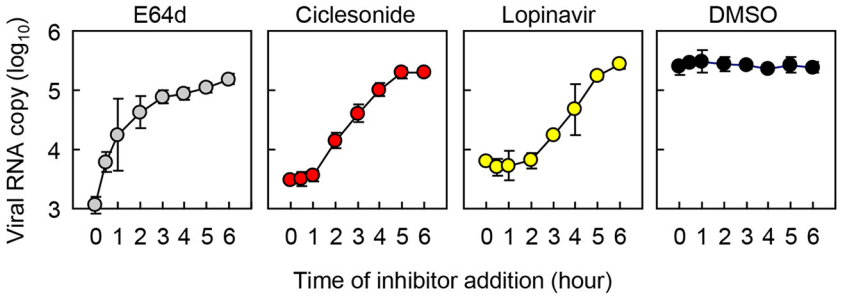

FIG 3 Time-of-addition assays for MERS-CoV replication inhibitors. The inhibitor E64d, ciclesonide, or lopinavir (each at 10 μM) or DMSO (control) was added to Vero cells at the indicated times after virus inoculation (MOI of 1). The amount of cellular viral mRNA at 6 h postinfection was measured by real-time PCR using a upE primer/probe set. Data are presented as the means ± SD from 4 independent experiments.

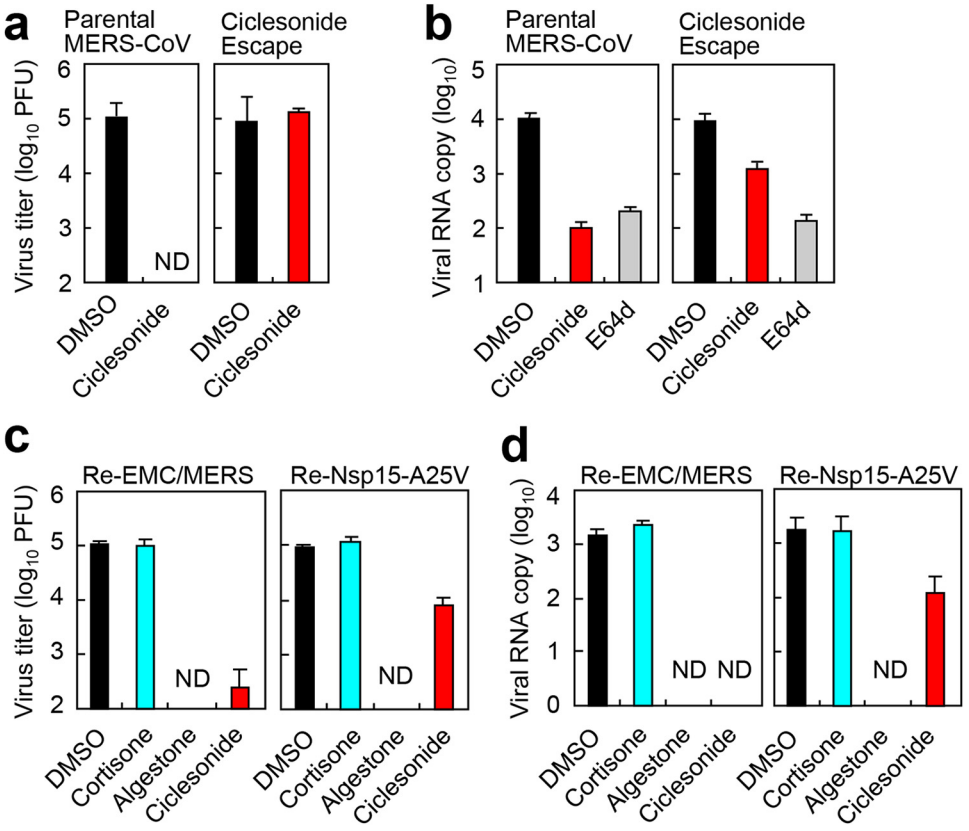

FIG 4 A ciclesonide escape mutant of MERS-CoV. (a) Viral growth of a ciclesonide escape mutant of MERS-CoV. Vero cells treated with 10 μM ciclesonide were infected with parental MERS-CoV or the ciclesonide escape mutant at an MOI of 0.01. The viral titer in the culture medium was quantified at 24 postinfection (hpi). (b) Viral RNA replication of a ciclesonide escape mutant of MERS-CoV. Vero cells treated with 10 μM ciclesonide were infected with parental MERS-CoV or the ciclesonide escape mutant at an MOI of 1. The viral RNA in the cells was quantified at 6 hpi. E64d (10 μM), a virus entry inhibitor, was used for comparison. (c) Growth of the recombinant virus. Vero cells were infected with the parental MERS-CoV/EMC strain (Re-EMC/MERS) or the recombinant mutant strain (Re-Nsp15-A25V) containing an amino acid substitution at A25V in nsp15 at an MOI of 0.01 and then treated with the indicated compounds (10 μM). The virus titer was quantified at 24 hpi. (d) RNA replication of the recombinant virus. Vero cells were infected with Re-EMC/MERS or Re-Nsp15-A25V at an MOI of 1 and treated with the indicated compounds (10 μM). The viral RNA in infected cells was quantified at 6 hpi. ND, not detected.

quently, a recombinant virus carrying the A25V amino acid substitution in nsp15 (Re-Nsp15-A25V) was generated from the parental MERS-CoV/EMC strain (Re-EMC/MERS) using a bacterial artificial chromosome (BAC) reverse-genetics system (19). The titer of recombinant virus in the culture medium of infected Vero cells at 24 hpi and the amount of viral RNA in cells at 6 hpi were quantified. As expected, the Re-Nsp15-A25V strain was much less susceptible to ciclesonide than the parental strain (Fig. 4c and d).

Antiviral effects of steroid compounds on SARS-CoV-2. In response to the global outbreak of COVID-19, we changed our study target from MERS-CoV to SARS-CoV-2. We then evaluated the inhibitory effects of ciclesonide on the replication of the latter. First, the effective concentration of ciclesonide required to inhibit virus propagation was assessed by quantifying the virus titer in the supernatant of VeroE6/*TMPRSS2* cells at 24 hpi (Fig. 5a and b); this cell line is highly susceptible to SARS-CoV-2 (20). We also examined human bronchial epithelial Calu-3 cells (Fig. 5c and d). Ciclesonide blocked SARS-CoV-2 replication in a concentration-dependent manner (50% effective concentration [EC_{90}] = 5.1 μM in VeroE6/*TMPRSS2* cells; EC_{90} = 6.0 μM in Calu-3 cells). In addition, differentiated primary human bronchial tracheal epithelial (HBTE) cells at an air-liquid interface (ALI) (HBTE/ALI cells) were prepared, and SARS-CoV-2 replication was evaluated. In untreated cells, we found a 2,000-fold increase in the amount of viral RNA at 3 days postinfection (Fig. 5e); at this time point, ciclesonide suppressed the replica-

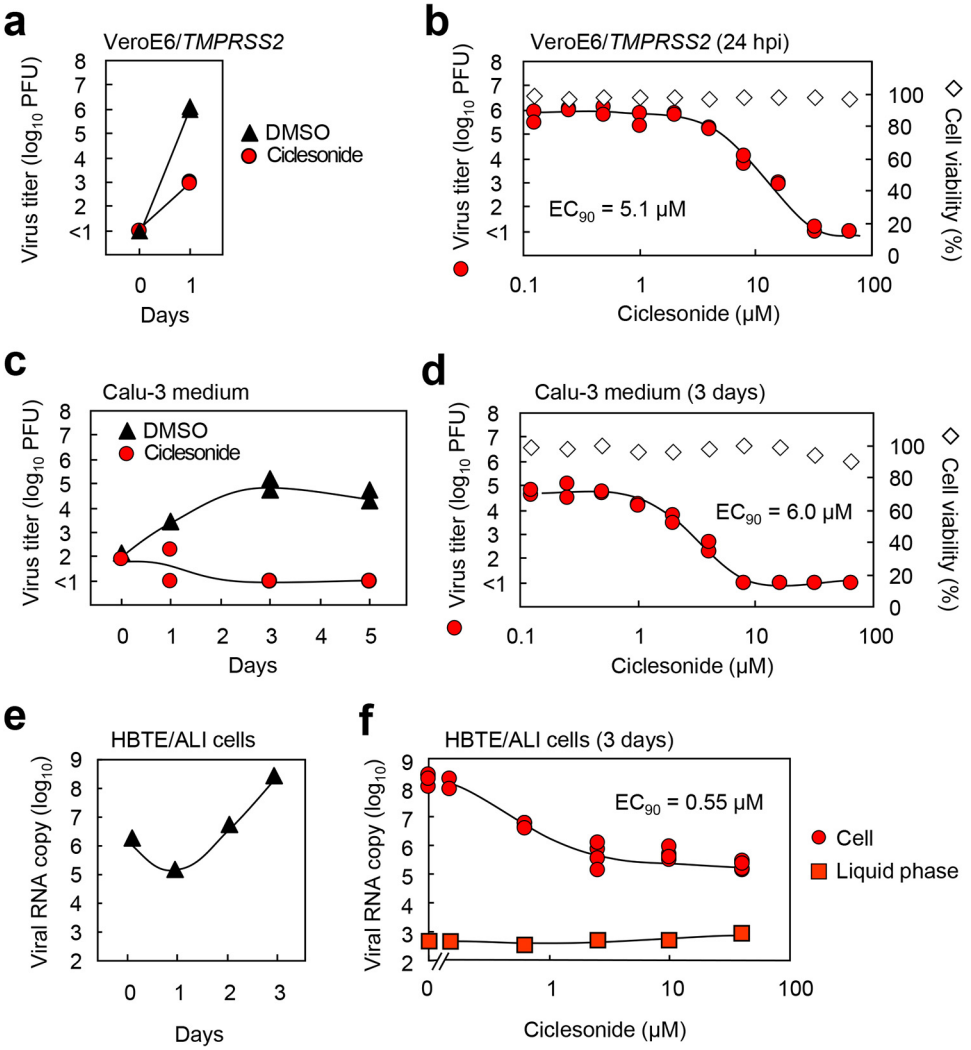

FIG 5 Ciclesonide suppresses the replication of SARS-CoV-2. (a, c, and e) Time course of SARS-CoV-2 propagation. (b, d, and f) Concentration-dependent effects of ciclesonide. VeroE6/*TMPRSS2* cells (a and b), Calu-3 cells (c and d), or HBTE/ALI cells (e and f) were infected with SARS-CoV-2 at an MOI of 0.001 in the presence of DMSO or ciclesonide (10 μM) and then incubated for 1, 3, or 5 days. The virus titer in medium was quantified by a plaque assay using VeroE6/*TMPRSS2* cells ($n = 2$ [a and c]); alternatively, the viral RNA in cells or culture medium was quantified by real-time PCR using the E gene primer/probe set ($n = 1$ [e] or $n = 4$ [f]). Average cell viability in the absence of virus was quantified using a WST assay ($n = 2$ [b and d]).

tion of viral RNA when used at a low concentration ($EC_{90} = 0.55$ μM in HBTE/ALI cells) (Fig. 5f). The amount of viral RNA detected in the liquid phase was small, indicating that less virus is secreted via the basolateral surface (Fig. 5f).

To assess the effect of ciclesonide at the early stage of SARS-CoV-2 replication, we measured the amount of viral RNA in VeroE6/*TMPRSS2* cells over time. Viral RNA replication was quantifiable at 6 h postinfection (Fig. 6a). Nelfinavir and lopinavir, strong inhibitors of SARS-CoV-2 RNA replication (4, 21), were compared with ciclesonide. At 6 hpi, mometasone and ciclesonide suppressed the replication of SARS-CoV-2 (MOI = 1) viral RNA with efficacies similar to those of nelfinavir and lopinavir; however, fluticasone and dexamethasone did not suppress viral replication (Fig. 6b).

Identification of the target of ciclesonide during SARS-CoV-2 replication. To identify the molecule targeted by ciclesonide to suppress viral RNA replication, we generated ciclesonide escape mutants. We could not technically identify a single point mutation from the multiple mutations revealed by next-generation sequencing after

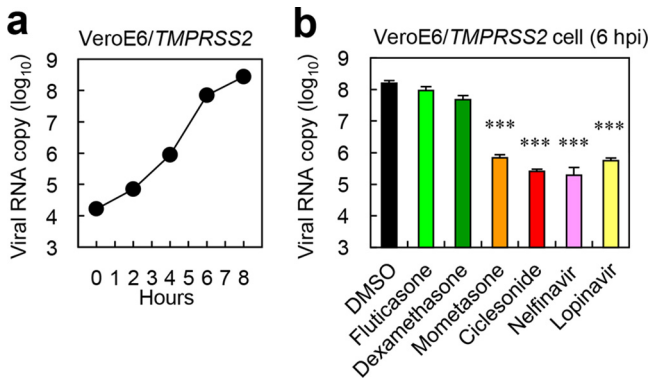

FIG 6 Steroid compounds and other inhibitors suppress SARS-CoV-2 RNA replication in VeroE6/*TMPRSS2* cells. (a) Time course of SARS-CoV-2 RNA replication. Cells were infected with virus at an MOI of 1, and cellular RNA was collected at the indicated time points. (b) Inhibition of viral RNA replication. Cells were infected with SARS-CoV-2 at an MOI of 1 in the presence of the indicated compounds (10 μM) for 6 h. Cellular viral RNA was quantified by real-time PCR using the E gene primer/probe set. ***, $P \leq 0.001$.

virus passage because no reverse-genetics system for SARS-CoV-2 was available in our laboratory. Therefore, we carried out virus passage using 43 SARS-CoV-2 isolates from infected patients to screen for ciclesonide escape mutants harboring a single point mutation. Thus, we carried out consecutive passages of these isolates in VeroE6/*TMPRSS2* cells in the presence of 40 μM ciclesonide. After eight passages, three viral plaques from each passage of the 43 cell supernatants were isolated in a limiting-dilution assay; the viral RNA was then isolated for next-generation sequencing. We obtained 15 isolates harboring a single mutation and 22 isolates harboring multiple mutations in the viral genome (compared with that of the parental virus) (Table 1 shows the mutations identified in 15 isolates). Next, we examined the replication of these mutants in the presence of ciclesonide. First, one of these isolates was tested in VeroE6/*TMPRSS2* cells. At 6 hpi, the amount of viral RNA derived from the parental virus fell by 1,000-fold in the presence of ciclesonide; in contrast, the amount of RNA derived from the escape mutant increased 50-fold compared with that of the parent virus (Fig. 7). There was no difference between the parental virus and the escape mutant in the presence of other steroid compounds (i.e., cortisone and algestone acetophenide) (Fig. 7). Furthermore, when we tested all 15 mutants in the presence of ciclesonide, we found a 6- to 50-fold increase in the amount of mutant viral RNA compared with that of the parental virus (Fig. 8a). Importantly, ciclesonide suppressed the replication of all escape mutants by ≥90%, suggesting that these mutants cannot completely overcome ciclesonide blockade. Mutations in the ciclesonide escape mutants were identified at three positions in nsp3 and at one position in nsp4 (Fig. 8b). Of note, the amino acid substitution N1543K in nsp3 was caused by a different base change (T7348G and T7348A) (Table 1). nsp3 and nsp4 are involved in the formation of double-membrane

TABLE 1 Mutations in the ciclesonide escape mutants

Coronavirus species, GenBank accession no. of reference sequence	Mutation in the viral genome	Amino acid position in ORF1a[a]	nsp, amino acid position	Passage no.	Parental strain(s) of mutant
MERS-CoV-2, NC_019843.3	C19647T	6457	nsp15, A25V	11	EMC/2012
SARS-CoV-2, MN908947.3	T7348G	2361	nsp3, N1543K	8	DP15-134, DP15-200, DP16-090, DP16-281, DP17-144
	T7348A	2361	nsp3, N1543K	8	WK-521
	G8006A	2581	nsp3, G1763S	8	DP15-078, DP15-196, DP16-074, DP16-157, DP16-282, DP17-187
	A8010C	2582	nsp3, D1764A	8	DP17-243
	G9242A	2994	nsp4, E230K	8	DP15-104, DP16-238

[a]ORF1a, open reading frame 1a.

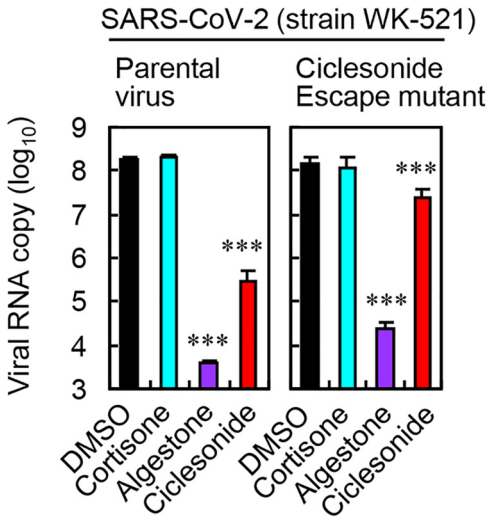

FIG 7 A ciclesonide escape mutant of SARS-CoV-2. VeroE6/*TMPRSS2* cells treated with the indicated compounds (each at 10 μM) were infected with parental SARS-CoV-2 or with the ciclesonide escape mutant (MOI = 1). Viral RNA titers in cells were measured at 6.5 hpi. Data are presented as the means ± SD from 4 independent experiments. ***, $P \leq 0.001$.

vesicles (DMVs), which anchor the coronavirus replication-transcription complex (RTC) within cells (22–24). In VeroE6/*TMPRSS2* cells, the distributions of double-stranded RNA (dsRNA) (a presumed intermediate during RNA synthesis localized to the DMV interior) and nsp3 were detected by specific antibodies at 5 hpi (Fig. 9). The fluorescence intensity of these molecules fell in the presence of ciclesonide in a concentration-dependent manner (Fig. 9). This result suggests that DMV formation might be inhibited directly by ciclesonide, but we cannot exclude the possibility that DMV formation was inhibited indirectly by interfering with another step of RNA replication, for example, relating to the function of nsp3, nsp4, or nsp15.

DISCUSSION

Inhaled ciclesonide is safe; indeed, it can be administered to infants at high concentrations. Because it remains primarily in lung tissue and does not enter the bloodstream to any significant degree (25), its immunosuppressive effects are weaker than those of cortisone and prednisolone (25, 26). In the preprint of this study (posted on bioRxiv), we showed that ciclesonide is a potent blocker of SARS-CoV-2 replication (27). Based on the data in our preprint study, clinical trials of a retrospective cohort study to treat COVID-19 patients were started in Japanese hospitals in March 2020. The treatment regime involves inhalation of 400 μg ciclesonide (two or three times per day; total, 1,200 μg/day) for 2 weeks. Three cases of COVID-19 pneumonia treated successfully with ciclesonide have been reported (28), as have several case reports (29–31). None of these studies reported significant side effects. The beneficial effects of ciclesonide in patients might be due to interference with viral replication and dampening of host inflammatory responses to infection in the lungs. The aim of the present study was to outline the scientific rationale for conducting these clinical trials.

Here, we show that ciclesonide suppresses the replication of coronaviruses, including betacoronaviruses (MHV-2, MERS-CoV, SARS-CoV, and SARS-CoV-2) and alphacoronaviruses (HCoV-229E), in cultured cells. Thus, ciclesonide is expected to be a broad-spectrum antiviral drug that is effective against many members of the coronavirus family. Indeed, it could be prescribed for the treatment of common colds, MERS, and COVID-19. The concentration of ciclesonide that effectively reduced the replication of SARS-CoV-2 in differentiated HBTE cells was 10-fold lower ($EC_{90} = 0.55$ μM) than that required to suppress replication in VeroE6/*TMPRSS2* or Calu-3 cells (Fig. 5b, d, and f). It is speculated that ciclesonide is a prodrug that is metabolized in lung tissue to yield the

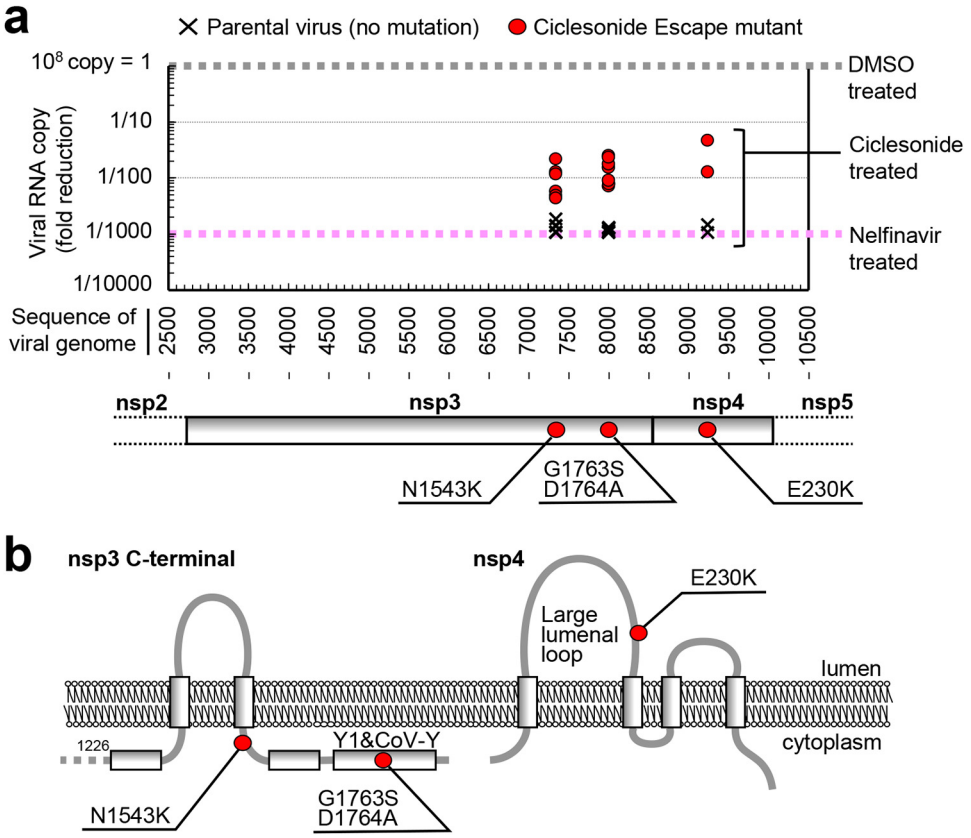

FIG 8 Amino acid substitutions in ciclesonide escape mutants of SARS-CoV-2. (a) Virus replication in the presence of ciclesonide (10 μM) is due to amino acid substitutions in nsp3 and nsp4. The replication of RNA derived from the 15 mutants listed in Table 1 was assessed in VeroE6/*TMPRSS2* cells. Viral RNA was isolated at 6 hpi and measured by real-time PCR using the E gene primer/probe set. The results were compared with those for the parental virus in which the viral RNA level after treatment with DMSO was set to 1 and that after treatment with nelfinavir was set to 1/1,000. Relative reductions of viral RNA in the presence of ciclesonide were plotted at the corresponding mutations in the SARS-CoV-2 genome sequence. Data are presented as the averages from two independent experiments. The amino acid substitutions in nsp3 and nsp4 are shown at the bottom. (b) Topological diagram. The C-terminal region of nsp3 and full-length nsp4 are depicted on the lipid bilayer of the endoplasmic reticulum membrane.

active form (32); therefore, it may be converted into its active form in differentiated HBTE cells. The EC_{90} for ciclesonide (0.55 μM) suggests that the administration of 1,200 μg/day to patients in clinical trials delivered a sufficient concentration of the drug to the lungs (because 0.55 μM is equivalent to 1,200 μg of ciclesonide dissolved in 4 liters of exudate fluid).

Furthermore, this study predicts the occurrence of ciclesonide escape mutants in patients treated with ciclesonide; however, the drug suppresses the replication of these mutants by >90% (Fig. 8a); of note, this finding is true for escape mutants of SARS-CoV-2, but it may not be the case for MERS-CoV. A ciclesonide escape mutant of MERS-CoV harbored an amino acid substitution at the dimerization site of the nsp15 homohexamer. nsp15 is a uridylate-specific endoribonuclease (NendoU), an RNA endonuclease, which plays a critical role in coronavirus replication (33, 34). Recently, an *in silico* study suggested a direct interaction between ciclesonide and nsp15 of SARS-CoV-2 (35). However, we did not identify mutations in nsp15 of the ciclesonide escape mutants of SARS-CoV-2; rather, we identified mutations in the C-terminal cytosolic region (next to the transmembrane domain or within the Y1 & CoV-Y domain) of nsp3 or in the large luminal loop of nsp4 (Fig. 8b), implying a potential difference between MERS-CoV and SARS-CoV-2. This also suggests the importance of carrying out virus passage in parallel (using many isolates in respective culture wells) to generate drug-resistant mutants. nsp3 contains a papain-like protease, and due to the large number

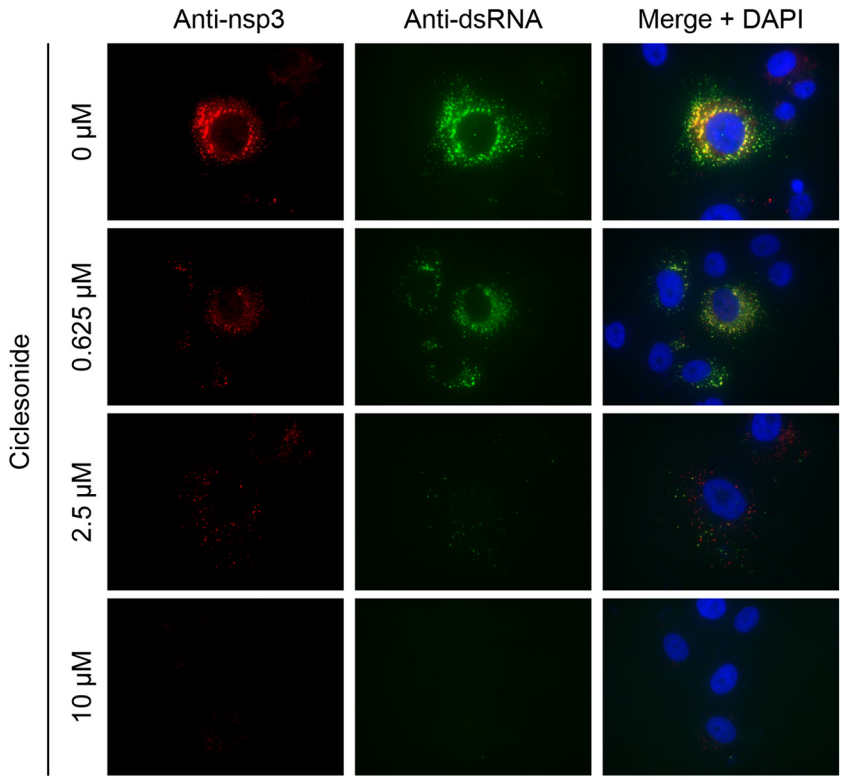

FIG 9 Distribution of nsp3 and double-strand RNA in the presence or absence of ciclesonide. VeroE6/*TMPRSS2* cells were infected with SARS-CoV-2 at an MOI of 0.1 in the presence of DMSO or ciclesonide and then incubated for 5 h. Next, cells were fixed with 4% paraformaldehyde and permeabilized with 0.1% Tween 20. nsp3 and double-strand RNA were stained with a rabbit anti-SARS-nsp4 antibody and a mouse anti-dsRNA antibody, followed by Alexa Fluor 594-conjugated anti-rabbit IgG and Alexa Fluor 488-conjugated anti-mouse IgG. Cell nuclei were stained with DAPI.

of interactions with other nsp's (including nsp4 and nsp15), it is believed to be part of the central scaffolding protein of the replication-transcription complex (34, 36, 37). Until now, the mutations identified in these mutants have not been detected in SARS-CoV-2 sequences in the GISAID and NCBI databases. In addition, previous studies show that passage of SARS-CoV-2 in VeroE6 cells results in mutations in the spike protein but not in nsp3 or nsp4 (38, 39). In our laboratory, no specific mutations in the SARS-CoV-2 genome have been observed after eight passages in VeroE6/*TMPRSS2* cells.

This study includes data showing that ciclesonide specifically blocks coronavirus replication, although the underlying molecular mechanism is not clear. Rubella virus, which has a positive-strand RNA genome and forms a spherule-like structure (like coronavirus DMVs) in cells, was suppressed slightly by ciclesonide, but influenza virus and RSV (which have negative-strand RNA genomes) were not, suggesting that ciclesonide may interact with an intracellular structure common to rubella and coronavirus replication. Additional experiments are needed to explain the mechanism of action of ciclesonide and whether it depends on the negative or positive strand of viral RNA. It is difficult to identify the mechanism by which ciclesonide targets the nsp complex because little is known about the construction and interaction of nsp's in the replication-transcription complex. The data in Fig. 9 do not ascertain whether DMV formation or RNA replication is inhibited first by ciclesonide. We anticipate that further experiments using mutant nsp's may reveal the molecular mechanism underlying the antiviral effect of ciclesonide.

MATERIALS AND METHODS

Cells and viruses. Hep-2, HeLa229, MDCK, Calu-3, Vero, Vero/*TMPRSS2*, and VeroE6/*TMPRSS2* cells were maintained in high-glucose Dulbecco's modified Eagle's medium (DMEM; Sigma-Aldrich, USA), and

TABLE 2 Primers and probes used for real-time PCR

Target	Method of detection	Primer or probe name	Sequence
MERS-CoV	Hybridization	EMC-Leader	CTCGTTCTCTTGCAGAACTTTG
		EMC-R	TGCCCAGGTGGAAAGGT
		EMC-FITC	AGCCCAGTGTACCAAGAGACAGTGTTATTTG
		EMC-LC	TGCAGCTCGTGGTTTTGGATTACGTCCT
MERS-CoV	TaqMan	upE-F	GCAACGCGCGATTCAGTT
		upE-R	GCCTCTACACGGGACCCATA
		upE-FAM	CTCTTCACATAATCGCCCCGAGCTCG
SARS-CoV	Hybridization	SARS-N-F	ACCAGAATGGAGGACGCAATGGGGCAAG
		SARS-N-R	TCTAAGTTCCTCCTTGCCAT
		SARS-N-FITC	ACCAGAATGGAGGACGCAATGGGGCAAG
		SARS-N-LC	CCAAAACAGCGCCGACCCCAAGGTTTAC
SARS-CoV-2	TaqMan	E_Sarbeco_F	ACAGGTACGTTAATAGTTAATAGCGT
		E_Sarbeco_R	ATATTGCAGCAGTACGCACACA
		E_Sarbeco_P1-FAM	ACACTAGCCATCCTTACTGCGCTTCG
HCoV-229E	TaqMan	229E-Lab-S-F	CGTTGACTTCAAACCTCAGA
		229E-Lab-S-R	ACCAACATTGGCATAAACAG
		229E-Lab-S-FAM	AGTTAAAGCACTTGCCACCGCC
MHV-2	Hybridization	MHV-N-F	TGTCTTTTGTTCCTGGGCA
		MHV-N-R	CAAGAGTAATGGGGAACCA
		MHV-N-FITC	GCTCCTCTGGAAACCGCGCTGGTAATGG
		MHV-N-LC	ATCCTCAAGAAGACCACTTGGGCTGACCAAACC
Rubella virus	TaqMan	RV(32–54)-F	CCTAHYCCCATGGAGAAACTCCT
		RV(143–160)-R	AACATCGCGCACTTCCCA
		RV(93–106)-FAM	CCGTCGGCAGTTGG
RSV	TaqMan	RSV-F	GGCAAATATGGAAACATACGTGAA
		RSV-R	TCTTTTTCTAGGACATTGTAYTGAACAG
		RSV-FAM	CTGTGTATGTGGAGCCTTCGTGAAGCT
Human GAPDH	SYBR	GAPDH-F	AGAACATCATCCCTGCCTCTACTG
		GAPDH-R	CCTCCGACGCCTGCTTCAC

DBT cells were maintained in DMEM (Nissui, Japan), supplemented with 5% fetal bovine serum (Gibco-BRL, USA). MERS-CoV and SARS-CoV-2 were propagated in Vero and VeroE6/*TMPRSS2* cells, respectively. HBTE cells (catalog number KH-4099; Lifeline Cell Technology, USA) were plated on 6.5-mm-diameter Transwell permeable supports (catalog number 3470; Corning, USA), and human airway epithelium cultures were generated by growing the cells at an air-liquid interface for 3 weeks, resulting in well-differentiated, polarized cultures. For the treatment of HBTE cells in the experiments, ciclesonide was mixed in liquid-phase medium at the indicated concentrations, and virus was inoculated onto the air phase.

Steroids and inhibitors. The following compounds were used: cortisone, prednisolone, fluticasone, dexamethasone, algestone acetophenide, mifepristone, mometasone furoate, and ciclesonide (all from the Prestwick Chemical Library; PerkinElmer, USA); E64d (catalog number 330005; Calbiochem, USA); nelfinavir (catalog number B1122; ApexBio, USA); and lopinavir (catalog number SML1222; Sigma-Aldrich).

Quantification of viral RNA. Confluent cells in 96-well plates were inoculated with virus in the presence of steroid compounds. Cellular RNA was isolated at 6 hpi using the CellAmp direct RNA prep kit (catalog number 3732; TaKaRa, Japan). The RNA was then diluted in water and boiled. Culture medium was collected at the indicated time points, diluted 10-fold in water, and then boiled. Real-time PCR assays to measure the amount of coronavirus RNA were performed using a MyGo Pro instrument (IT-IS Life Science, Ireland). The primers and probes are described in Table 2. Viral mRNA levels were normalized to the expression levels of the cellular housekeeping gene glyceraldehyde-3-phosphate dehydrogenase (GAPDH).

Cytotoxicity assays. Confluent cells in 96-well plates were treated with steroid compounds. After incubation for 24 or 27 h, a cell viability assay was performed using WST reagent (catalog number CK12; Dojin Lab, Japan), according to the manufacturer's instructions.

Generation of recombinant MERS-CoV from BAC plasmids. A BAC clone carrying the full-length infectious genome of the MERS-CoV EMC2012 strain, pBAC-MERS-wt, was used to generate recombinant MERS-CoV, as described previously (19, 40). The BAC DNA of SARS-CoV-Rep (41), kindly provided by Luis Enjuanes, was used as a backbone BAC sequence to generate pBAC-MERS-wt. The BAC infectious clones carrying amino acid substitutions in nsp15 were generated by modification of pBAC-MERS-wt (as a

template) using a Red/ET recombination system counterselection BAC modification kit (Gene Bridges, Heidelberg, Germany). BHK-21 cells were grown in a single well of a 6-well plate in 10% fetal calf serum (FCS)–minimal essential medium (MEM) and transfected with 3 μg BAC plasmid using Lipofectamine 3000 (Thermo Fisher, USA). After transfection, Vero/*TMPRSS2* cells were inoculated onto transfected BHK-21 cells. The coculture was then incubated at 37°C for 3 days. The supernatants were collected and propagated once in Vero/*TMPRSS2* cells. Recovered viruses were stored at −80°C.

Generation of ciclesonide escape mutants. To obtain ciclesonide escape mutants, virus passage was repeated at least eight times in the presence of 40 μM ciclesonide. At the first passage, about 10^7 PFU of virus was inoculated onto 10^6 cells and incubated for 3 h. Next, the cells were washed twice with culture medium and incubated for 2 days in the presence of ciclesonide. The incubation periods were 2 days for the first three passages and 1 day for the following passages. Cells were inoculated with 100 μl culture medium at each successive passage. The amount of replicating virus in the presence of ciclesonide was quantified using real-time PCR. Vero and VeroE6/*TMPRSS2* cells were used to passage MERS-CoV and SARS-CoV-2, respectively.

Whole-genome sequencing of SARS-CoV-2. Extracted viral RNA was reverse transcribed and tagged with index adaptors using the NEBNext Ultra II RNA library prep kit for Illumina (New England Biolabs, Ipswich, MA, USA), according to the manufacturer's instructions. The resulting cDNA libraries were verified using the MultiNA system (Shimadzu, Kyoto, Japan) and quantified using a Quantus fluorometer (Promega, Madison, WI, USA). Indexed libraries were then converted and sequenced (150-bp paired-end reads) using the DNBSEQ-G400 system (MGI Tech, Shenzhen, China; operated by Genewiz, South Plainfield, NJ, USA). After sequencing, reads with the same index sequences were grouped. Sequence reads were trimmed by Ktrim (42) and mapped onto the viral genomes of parental strains using Minimap2 (43). The consensus sequences of the mapped reads were obtained using ConsensusFixer (A. Töpfer [https://github.com/cbg-ethz/consensusfixer]).

Immunofluorescence microscopy. VeroE6/*TMPRSS2* cells cultured on 96-well plates (Lumos multiwell 96, catalog number 94 6120 096; Sarstedt AG & Co. KG, Germany) were infected with SARS-CoV-2 (WK-521) at an MOI of 0.1 and incubated for 5 h. Next, the cells were fixed for 30 min at 4°C with 4% paraformaldehyde in phosphate-buffered saline (PBS). After washing once with PBS, the cells were permeabilized for 15 min at room temperature (RT) with PBS containing 0.1% Tween 20. The cells were then incubated with a mixture of rabbit anti-SARS-nsp4 (1:500) (catalog number ab181620; Abcam, USA) and mouse anti-dsRNA (1:1,000) (catalog number J2-1709; Scicons, Hungary) antibodies for 1 h at RT, washed three times with PBS, and incubated for 1 h at RT with a mixture of Alexa Fluor 594-conjugated anti-rabbit IgG (1:500) (catalog number A11012; Thermo Fisher) and Alexa Fluor 488-conjugated anti-mouse IgG (1:500) (catalog number A10680; Thermo Fisher). Next, the cells were washed three times with PBS, and cell nuclei were stained with 4′,6-diamidino-2-phenylindole (DAPI) (1:5,000) (catalog number D1306; Thermo Fisher). Cells were observed under an inverted fluorescence phase-contrast microscope (catalog number BZ-X810; Keyence, Japan).

Statistical analysis. Statistical significance was assessed using analyses of variance (ANOVAs). A P value of <0.05 was considered statistically significant. In figures with error bars, data are presented as the means ± standard deviations (SD).

ACKNOWLEDGMENTS

We are most grateful to Tsuneo Morishima (Aichi Medical University) for helpful suggestions. We also thank Yuriko Tomita, Makoto Kuroda, Tsuyoshi Sekizuka, Ikuyo Takayama, Mina Nakauchi, Kazuya Nakamura, Tsutomu Kageyama, Kazuhiko Kanou, Kiyoko Okamoto, Naoko Iwata, and Noriyo Nagata (National Institute of Infectious Diseases) for providing reagents and important information; Ron A. M. Fouchier and Bart L. Haagmans (Erasmus Medical Center) for providing MERS-CoV; and John Ziebuhr (University of Wurzburg) for providing SARS-CoV.

This study was supported by grants-in-aid from the Japan Agency for Medical Research and Development (AMED) (grant numbers JP19fk0108058j0802 and 20fk0108058j0803) and from the Japan Society for the Promotion of Science (JSPS) (grant numbers 17K08868 and 20K07519).

REFERENCES

1. Zhu N, Zhang D, Wang W, Li X, Yang B, Song J, Zhao X, Huang B, Shi W, Lu R, Niu P, Zhan F, Ma X, Wang D, Xu W, Wu G, Gao GF, Tan W, China Novel Coronavirus Investigating and Research Team. 2020. A novel coronavirus from patients with pneumonia in China, 2019. N Engl J Med 382:727–733. https://doi.org/10.1056/NEJMoa2001017.
2. Lu H. 2020. Drug treatment options for the 2019-new coronavirus (2019-nCoV). Biosci Trends 14:69–71. https://doi.org/10.5582/bst.2020.01020.
3. Wang M, Cao R, Zhang L, Yang X, Liu J, Xu M, Shi Z, Hu Z, Zhong W, Xiao G. 2020. Remdesivir and chloroquine effectively inhibit the recently emerged novel coronavirus (2019-nCoV) in vitro. Cell Res 30:269–271. https://doi.org/10.1038/s41422-020-0282-0.
4. Jeon S, Ko M, Lee J, Choi I, Byun SY, Park S, Shum D, Kim S. 2020. Identification of antiviral drug candidates against SARS-CoV-2 from FDA-approved drugs. Antimicrob Agents Chemother 64:e00819-20. https://doi.org/10.1128/AAC.00819-20.
5. Beigel JH, Tomashek KM, Dodd LE, Mehta AK, Zingman BS, Kalil AC, Hohmann E, Chu HY, Luetkemeyer A, Kline S, Lopez de Castilla D, Finberg RW, Dierberg K, Tapson V, Hsieh L, Patterson TF, Paredes R, Sweeney DA, Short WR, Touloumi G, Lye DC, Ohmagari N, Oh M-D, Ruiz-Palacios GM, Benfield

T, Fätkenheuer G, Kortepeter MG, Atmar RL, Creech CB, Lundgren J, Babiker AG, Pett S, Neaton JD, Burgess TH, Bonnett T, Green M, Makowski M, Osinusi A, Nayak S, Lane HC, ACTT-1 Study Group. 8 October 2020. Remdesivir for the treatment of Covid-19—final report. N Engl J Med https://doi.org/10.1056/NEJMoa2007764.

6. Wang Y, Zhang D, Du G, Du R, Zhao J, Jin Y, Fu S, Gao L, Cheng Z, Lu Q, Hu Y, Luo G, Wang K, Lu Y, Li H, Wang S, Ruan S, Yang C, Mei C, Wang Y, Ding D, Wu F, Tang X, Ye X, Ye Y, Liu B, Yang J, Yin W, Wang A, Fan G, Zhou F, Liu Z, Gu X, Xu J, Shang L, Zhang Y, Cao L, Guo T, Wan Y, Qin H, Jiang Y, Jaki T, Hayden FG, Horby PW, Cao B, Wang C. 2020. Remdesivir in adults with severe COVID-19: a randomised, double-blind, placebo-controlled, multicentre trial. Lancet 395:1569–1578. https://doi.org/10.1016/S0140-6736(20)31022-9.
7. Cao B, Wang Y, Wen D, Liu W, Wang J, Fan G, Ruan L, Song B, Cai Y, Wei M, Li X, Xia J, Chen N, Xiang J, Yu T, Bai T, Xie X, Zhang L, Li C, Yuan Y, Chen H, Li H, Huang H, Tu S, Gong F, Liu Y, Wei Y, Dong C, Zhou F, Gu X, Xu J, Liu Z, Zhang Y, Li H, Shang L, Wang K, Li K, Zhou X, Dong X, Qu Z, Lu S, Hu X, Ruan S, Luo S, Wu J, Peng L, Cheng F, Pan L, Zou J, Jia C, et al. 2020. A trial of lopinavir-ritonavir in adults hospitalized with severe Covid-19. N Engl J Med 382:1787–1799. https://doi.org/10.1056/NEJMoa2001282.
8. WHO. 2020. WHO discontinues hydroxychloroquine and lopinavir/ritonavir treatment arms for COVID-19. WHO news release. WHO, Geneva, Switzerland.
9. Kawashima H, Togashi T, Yamanaka G, Nakajima M, Nagai M, Aritaki K, Kashiwagi Y, Takekuma K, Hoshika A. 2005. Efficacy of plasma exchange and methylprednisolone pulse therapy on influenza-associated encephalopathy. J Infect 51:E53–E56. https://doi.org/10.1016/j.jinf.2004.08.017.
10. Baris HE, Baris S, Karakoc-Aydiner E, Gokce I, Yildiz N, Cicekkoku D, Ogulur I, Ozen A, Alpay H, Barlan I. 2016. The effect of systemic corticosteroids on the innate and adaptive immune system in children with steroid responsive nephrotic syndrome. Eur J Pediatr 175:685–693. https://doi.org/10.1007/s00431-016-2694-x.
11. Coutinho AE, Chapman KE. 2011. The anti-inflammatory and immunosuppressive effects of glucocorticoids, recent developments and mechanistic insights. Mol Cell Endocrinol 335:2–13. https://doi.org/10.1016/j.mce.2010.04.005.
12. Alfaraj SH, Al-Tawfiq JA, Assiri AY, Alzahrani NA, Alanazi AA, Memish ZA. 2019. Clinical predictors of mortality of Middle East respiratory syndrome coronavirus (MERS-CoV) infection: a cohort study. Travel Med Infect Dis 29:48–50. https://doi.org/10.1016/j.tmaid.2019.03.004.
13. Lee N, Allen Chan KC, Hui DS, Ng EKO, Wu A, Chiu RWK, Wong VWS, Chan PKS, Wong KT, Wong E, Cockram CS, Tam JS, Sung JJY, Lo YMD. 2004. Effects of early corticosteroid treatment on plasma SARS-associated coronavirus RNA concentrations in adult patients. J Clin Virol 31:304–309. https://doi.org/10.1016/j.jcv.2004.07.006.
14. Kawase M, Shirato K, van der Hoek L, Taguchi F, Matsuyama S. 2012. Simultaneous treatment of human bronchial epithelial cells with serine and cysteine protease inhibitors prevents severe acute respiratory syndrome coronavirus entry. J Virol 86:6537–6545. https://doi.org/10.1128/JVI.00094-12.
15. Nukoolkarn V, Lee VS, Malaisree M, Aruksakulwong O, Hannongbua S. 2008. Molecular dynamic simulations analysis of ritronavir [*sic*] and lopinavir as SARS-CoV 3CLpro inhibitors. J Theor Biol 254:861–867. https://doi.org/10.1016/j.jtbi.2008.07.030.
16. Athmer J, Fehr AR, Grunewald M, Smith EC, Denison MR, Perlman S. 2017. In situ tagged nsp15 reveals interactions with coronavirus replication/transcription complex-associated proteins. mBio 8:e002320-16. https://doi.org/10.1128/mBio.02320-16.
17. Deng X, Hackbart M, Mettelman RC, O'Brien A, Mielech AM, Yi G, Kao CC, Baker SC. 2017. Coronavirus nonstructural protein 15 mediates evasion of dsRNA sensors and limits apoptosis in macrophages. Proc Natl Acad Sci U S A 114:E4251–E4260. https://doi.org/10.1073/pnas.1618310114.
18. Lundin A, Dijkman R, Bergström T, Kann N, Adamiak B, Hannoun C, Kindler E, Jónsdóttir HR, Muth D, Kint J, Forlenza M, Müller MA, Drosten C, Thiel V, Trybala E. 2014. Targeting membrane-bound viral RNA synthesis reveals potent inhibition of diverse coronaviruses including the Middle East respiratory syndrome virus. PLoS Pathog 10:e1004166. https://doi.org/10.1371/journal.ppat.1004166.
19. Terada Y, Kawachi K, Matsuura Y, Kamitani W. 2017. MERS coronavirus nsp1 participates in an efficient propagation through a specific interaction with viral RNA. Virology 511:95–105. https://doi.org/10.1016/j.virol.2017.08.026.
20. Matsuyama S, Nao N, Shirato K, Kawase M, Saito S, Takayama I, Nagata N, Sekizuka T, Katoh H, Kato F, Sakata M, Tahara M, Kutsuna S, Ohmagari N, Kuroda M, Suzuki T, Kageyama T, Takeda M. 2020. Enhanced isolation of SARS-CoV-2 by TMPRSS2-expressing cells. Proc Natl Acad Sci U S A 117:7001–7003. https://doi.org/10.1073/pnas.2002589117.
21. Yamamoto N, Matsuyama S, Hoshino T, Yamamoto N. 2020. Nelfinavir inhibits replication of severe acute respiratory syndrome coronavirus 2 in vitro. bioRxiv.
22. Hagemeijer MC, Monastyrska I, Griffith J, van der Sluijs P, Voortman J, van Bergen en Henegouwen PM, Vonk AM, Rottier PJM, Reggiori F, De Haan CAM. 2014. Membrane rearrangements mediated by coronavirus nonstructural proteins 3 and 4. Virology 458–459:125–135. https://doi.org/10.1016/j.virol.2014.04.027.
23. Sakai Y, Kawachi K, Terada Y, Omori H, Matsuura Y, Kamitani W. 2017. Two-amino acids change in the nsp4 of SARS coronavirus abolishes viral replication. Virology 510:165–174. https://doi.org/10.1016/j.virol.2017.07.019.
24. Wolff G, Limpens RWAL, Zevenhoven-Dobbe JC, Laugks U, Zheng S, de Jong AWM, Koning RI, Agard DA, Grünewald K, Koster AJ, Snijder EJ, Bárcena M. 2020. A molecular pore spans the double membrane of the coronavirus replication organelle. Science 369:1395–1398. https://doi.org/10.1126/science.abd3629.
25. Lee DKC, Fardon TC, Bates CE, Haggart K, McFarlane LC, Lipworth BJ. 2005. Airway and systemic effects of hydrofluoroalkane formulations of high-dose ciclesonide and fluticasone in moderate persistent asthma. Chest 127:851–860. https://doi.org/10.1378/chest.127.3.851.
26. Lipworth BJ, Kaliner MA, LaForce CF, Baker JW, Kaiser HB, Amin D, Kundu S, Williams JE, Engelstaetter R, Banerji DD. 2005. Effect of ciclesonide and fluticasone on hypothalamic-pituitary-adrenal axis function in adults with mild-to-moderate persistent asthma. Ann Allergy Asthma Immunol 94:465–472. https://doi.org/10.1016/S1081-1206(10)61117-9.
27. Matsuyama S, Kawase M, Nao N, Shirato K, Ujike M, Kamitani W, Shimojima M, Fukushi S. 2020. The inhaled corticosteroid ciclesonide blocks coronavirus RNA replication by targeting viral NSP15. bioRxiv.
28. Iwabuchi K, Yoshie K, Kurakami Y, Takahashi K, Kato Y, Morishima T. 2020. Therapeutic potential of ciclesonide inhalation for COVID-19 pneumonia: report of three cases. J Infect Chemother 26:625–632. https://doi.org/10.1016/j.jiac.2020.04.007.
29. Nakajima K, Ogawa F, Sakai K, Uchiyama M, Oyama Y, Kato H, Takeuchi I. 2020. A case of coronavirus disease 2019 treated with ciclesonide. Mayo Clin Proc 95:1296–1297. https://doi.org/10.1016/j.mayocp.2020.04.007.
30. Yamasaki Y, Ooka S, Tsuchida T, Nakamura Y, Hagiwara Y, Naitou Y, Ishibashi Y, Ikeda H, Sakurada T, Handa H, Nishine H, Takita M, Morikawa D, Yoshida H, Fujii S, Morisawa K, Takemura H, Fujitani S, Kunishima H. 3 July 2020. The peripheral lymphocyte count as a predictor of severe COVID-19 and the effect of treatment with ciclesonide. Virus Res https://doi.org/10.1016/j.virusres.2020.198089.
31. Baba H, Kanamori H, Oshima K, Seike I, Niitsuma-Sugaya I, Takei K, Sato Y, Tokuda K, Aoyagi T. 2020. Prolonged presence of SARS-CoV-2 in a COVID-19 case with rheumatoid arthritis taking iguratimod treated with ciclesonide. J Infect Chemother 26:1100–1103. https://doi.org/10.1016/j.jiac.2020.06.022.
32. Nave R, Watz H, Hoffmann H, Boss H, Magnussen H. 2010. Deposition and metabolism of inhaled ciclesonide in the human lung. Eur Respir J 36:1113–1119. https://doi.org/10.1183/09031936.00172309.
33. Zhang L, Li L, Yan L, Ming Z, Jia Z, Lou Z, Rao Z. 2018. Structural and biochemical characterization of endoribonuclease Nsp15 encoded by Middle East respiratory syndrome coronavirus. J Virol 92:e00893-18. https://doi.org/10.1128/JVI.00893-18.
34. Kindler E, Gil-Cruz C, Spanier J, Li Y, Wilhelm J, Rabouw HH, Züst R, Hwang M, V'kovski P, Stalder H, Marti S, Habjan M, Cervantes-Barragan L, Elliot R, Karl N, Gaughan C, van Kuppeveld FJM, Silverman RH, Keller M, Ludewig B, Bergmann CC, Ziebuhr J, Weiss SR, Kalinke U, Thiel V. 2017. Early endonuclease-mediated evasion of RNA sensing ensures efficient coronavirus replication. PLoS Pathog 13:e1006195. https://doi.org/10.1371/journal.ppat.1006195.
35. Kimura H, Kurusu H, Sada M, Kurai D, Murakami K, Kamitani W, Tomita H, Katayama K, Ryo A. 2020. Molecular pharmacology of ciclesonide against SARS-CoV-2. J Allergy Clin Immunol 146:330–331. https://doi.org/10.1016/j.jaci.2020.05.029.
36. Lei J, Kusov Y, Hilgenfeld R. 2018. Nsp3 of coronaviruses: structures and functions of a large multi-domain protein. Antiviral Res 149:58–74. https://doi.org/10.1016/j.antiviral.2017.11.001.
37. Deng X, Baker SC. 2018. An "old" protein with a new story: coronavirus

endoribonuclease is important for evading host antiviral defenses. Virology 517:157–163. https://doi.org/10.1016/j.virol.2017.12.024.
38. Liu Z, Zheng H, Lin H, Li M, Yuan R, Peng J, Xiong Q, Sun J, Li B, Wu J, Yi L, Peng X, Zhang H, Zhang W, Hulswit RJG, Loman N, Rambaut A, Ke C, Bowden TA, Pybus OG, Lu J. 2020. Identification of common deletions in the spike protein of SARS-CoV-2. J Virol 94:e00790-20. https://doi.org/10.1128/JVI.00790-20.
39. Ogando NS, Dalebout TJ, Zevenhoven-Dobbe JC, Limpens RWAL, van der Meer Y, Caly L, Druce J, de Vries JJC, Kikkert M, Bárcena M, Sidorov I, Snijder EJ. 2020. SARS-coronavirus-2 replication in Vero E6 cells: replication kinetics, rapid adaptation and cytopathology. J Gen Virol 101:925–940. https://doi.org/10.1099/jgv.0.001453.
40. Almazán F, DeDiego ML, Sola I, Zuñiga S, Nieto-Torres JL, Marquez-Jurado S, Andrés G, Enjuanes L. 2013. Engineering a replication-competent, propagation-defective Middle East respiratory syndrome coronavirus as a vaccine candidate. mBio 4:e00650-13. https://doi.org/10.1128/mBio.00650-13.
41. Almazán F, DeDiego ML, Galán C, Escors D, Álvarez E, Ortego J, Sola I, Zuñiga S, Alonso S, Moreno JL, Nogales A, Capiscol C, Enjuanes L. 2006. Construction of a severe acute respiratory syndrome coronavirus infectious cDNA clone and a replicon to study coronavirus RNA synthesis. J Virol 80:10900–10906. https://doi.org/10.1128/JVI.00385-06.
42. Sun K. 2020. Ktrim: an extra-fast and accurate adapter- and quality-trimmer for sequencing data. Bioinformatics 36:3561–3562. https://doi.org/10.1093/bioinformatics/btaa171.
43. Li H. 2018. Minimap2: pairwise alignment for nucleotide sequences. Bioinformatics 34:3094–3100. https://doi.org/10.1093/bioinformatics/bty191.